In: Graphite
Editor: Quinton C. Campbell
ISBN: 978-1-62618-576-0

Chapter 10

ETHYLENE-OCTENE COPOLYMER/GRAPHITE COMPOSITES: ELECTRICAL AND THERMAL CONDUCTIVITIES AND FLAME RESISTANCE

***Petr Svoboda*[1,2*]**

[1] Department of Polymer Engineering, Faculty of Technology,
Tomas Bata University in Zlin, Zlin, Czech Republic
[2] Centre of Polymer Systems, University Institute,
Tomas Bata University in Zlin, Zlin, Czech Republic.

ABSTRACT

A series of ethylene-octene copolymer (EOC) composites have been prepared by melt-mixing with different weight ratios of expandable graphite filler (0-50% by weight). Electrical conductivity [both alternating current (AC) and direct current (DC)] and thermal conductivity studies were carried out.

Effect of filler loading and frequency on electrical conductivity was studied. DC conductivity has increased from 1.51×10^{-13} Scm^{-1} to 1.17×10^{-1} Scm^{-1}. Percolation threshold by DC and also AC methods was observed at about 16 vol. % of the filler. Real part of permittivity was found to be decreasing with increase in frequency while conductivity was increasing.

Thermal conductivity was also found to be increasing gradually from 0.196 to 0.676 $Wm^{-1}K^{-1}$ which is about 245% increase. Graphite not only increases the electrical and thermal conductivities but at and above 40 wt. %, also acts as a halogen-free, environmental friendly flame retardant. Horizontal burn rate was studied in detail with interesting results.

Initially the addition of graphite increases the horizontal burn rate but above 35 wt. % of graphite the burning speed decreases. Shore-A hardness of EOC/graphite composites shows that even with high graphite loading, the hardness is increased from about 50 to 68 only so that the rubbery nature of the composite is not affected very much.

* E-mail: svoboda@ft.utb.cz.

INTRODUCTION

Polymer composites with conducting fillers serve as electrical or thermal conductors and have wide range of applications in the electric and electronic fields. These composites have an advantage of conductivity of a filler and favorable properties of polymer material together. They are widely used in many areas like electrodes, separators, electromagnetic shielding and anti-static coating [1, 2]. The fillers generally subjected for conductivity studies are carbon fibers [3, 4], multi-wall carbon nanotubes (MWCNT) [5], natural fibers e.g. sisal fibers [6], expanded graphite [7], carbon black [8] and graphene [9].

Ethylene-octene copolymer (EOC) is a new type of copolymer developed by The Dow Chemical Company through constrained geometry catalyst technology (CGCT) under the trade name ENGAGE®. It is being considered for use in diverse applications such as cushioning agents, gaskets, and is particularly good alternative for sealing application due to its structural regularity and non-toxic composition. Several researchers have studied the conductivity properties of EOC composites using different fillers such as carbon black, polyaniline, and multi-wall carbon nanotubes [10-12]. Conducting polymer composites (CPC) with elastomeric polymer matrices have applications in the field of sensors, e.g. temperature sensors [13] and strain sensors [14].

Charge transport in polymer composite materials has been the object of many researches in the past. Conducting mechanism in composites containing conductive particles can be described by percolation theory [15]. The volume fraction of fillers above which the continuous conducting paths are created is known as percolation threshold. At this level, a continuous chain of particles in the matrix results in a considerable increase in conductivity of several orders. Conductivity above percolation threshold increases sharply and composites start behaving like semiconductors [16-19].

Permittivity is the ability of a material to store charge when used as a dielectric material. Capacitance and conductance as a function of frequency can be measured by dielectric analysis which can be then utilized to calculate real part (ε') and imaginary part (ε'') of permittivity and the dielectric loss factor ($\tan \delta$) [20].

Extensive studies have been performed on conductivity of numerous composites with different polymers as matrix and various fillers. Several researchers prepared composites by the incorporation of halogen-free flame retardant expandable graphite for the improvement of flame retardancy and thermal stability [21-24]. Expandable graphite as a conducting filler has been studied only few times [25, 26]. Only few researchers performed the conductivity studies using EOC as a matrix [10, 12]. In this paper, electrical and thermal conductivities of EOC/expandable graphite composites have been studied. Also, flame retardancy according to UL-94 (Underwriters Laboratories) horizontal test was evaluated.

MATERIALS AND METHODS

Materials

Ethylene-octene copolymer was Engage 8842 supplied by Dow Chemicals. The octene content was 45 wt. %, density = 0.8595 g cm^{-3} and melt flow index (MFI) = 1.02 dg min^{-1} (at

190°C /2.16 kg). Expandable graphite flakes were Grafguard 160-50N, used as received from Graftech Inc., Ohio, Cleaveland, USA. Mean particle size was 350 μm and density was about 2 g cm^{-3}.

Composite and Sample Preparation

EOC and Grafguard 160-50N were melt-mixed in a BrabenderPlasti-corder PL2000 mixing machine with a mixing volume of 50 cm^3 at 100 °C at mixing speed 50 rpm for 10 minutes. Graphite was preheated in a hot air oven at 100 °C for 12 h to remove any absorbed moisture. Graphite content was: 5, 10, 15, 20, 25, 30, 35, 40, 45, 50 wt. % or 2, 5, 7, 10, 13, 16, 19, 22, 26, 30 vol.%, respectively.

The melt-mixed composites were then compression molded to 2 mm thick sheets at 110 °C. From this sheet two discs were cut out: for the electrical conductivity measurement the disc had diameter 15 mm and for the thermal conductivity measurement it was 50 mm. Samples for flammability tests were cut out of the sheet according to UL-94 standard with sample dimensions being 125x13x2 mm. For shore-A hardness measurements the discs had diameter 50 mm and thickness 6 mm.

Scanning Electron Microscopy (SEM)

Morphology of the expandable graphite filler and composites was studied by using SEM technique. SEM analysis was carried out using Vega II LMU (Tescan, Czech Republic) with a beam acceleration voltage set at 10 kV.

Direct current (DC) Conductivity

The current-voltage dependencies were measured in the two-point setup using electrodes of cylindrical shape (13 mm in diameter and covered by a layer of gold) with a programmable electrometer (Keithley6517 A, USA).

The DC conductivity was calculated from the current–voltage dependence in the range of 1–20 V. Current-Voltage characteristics were measured in DC field. Specific electrical conductivity, σ_{DC}, can be expressed as follows:

$$\sigma_{DC} = \frac{I}{U} \cdot \frac{d}{A} \tag{1}$$

where, I is the electrical current, U is the voltage, A is area of electrodes and d is the thickness of the sample.

Four-point method (Van der Pauw) [27] was used for the measurement of samples with conductivity higher than 10^{-3} S cm^{-1}. A main advantage of four-probe measurements is the elimination of contact resistance [28]. All the properties were measured at room temperature (22-25 °C).

Dielectric Properties and Alternating Current (AC) Conductivity

Dielectric characteristics involving the frequency dependence of the real part (dielectric constant, ε') and imaginary part of the complex permittivity (dielectric loss, ε'') in the frequency range of 1 MHz – 3 GHz were determined with an Radio Frequency (RF) Impedance Analyzer (Agilent E4991A, USA) using capacitive method (on a dielectric material test fixture which comes furnished with the device). After inputting the sample thickness the device automatically calculates and yields frequency dependence of complex permittivity ε^*. In the range of 10 Hz-100 KHz, dielectric characteristics were measured by using Hioky 3522 (LCR Hi Tester, Japan). The dielectric constant was calculated from the measured capacitance.

AC conductivity, σ_{AC}, was calculated from imaginary part of complex permittivity, ε'', which was directly obtained from the instrument, following the equation (2):

$$\sigma_{AC} = 2\pi f \cdot \varepsilon_0 \cdot \varepsilon'' \tag{2}$$

where, ε_0 is permittivity of vacuum and *f is* frequency.

Thermal Conductivity

Thermal conductivity of EOC/graphite composites was measured according to Fitch (1935) [29] where the sample is sandwiched between a heat source insulated on all faces but one and a constant temperature brass cylinder as heat sink, as shown in Figure 1.The advantage of this approach is most of all short time of measurement and also the simplicity of the procedure and also the simplicity of the measuring instrument. During the quasisteady heat conductivity measurement, the temperature at certain place changes with time.

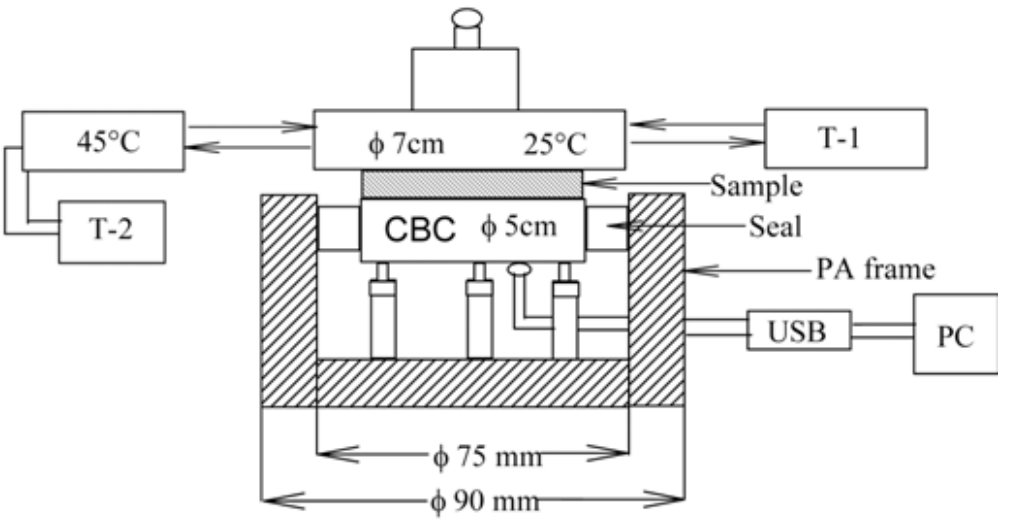

Figure 1. Schematic diagram of the apparatus used for thermal conductivity measurement.

The common procedure involves a case when the heat flows only in one direction. Then temperature depends only on time and one coordinate. This instrument is usually used for the measurement of thermal conductivity of thin sheets or slabs from various plastics and rubber and also for leather. The principle of measuring instrument and the procedure is explained below. Initially the central brass cylinder (CBC) with diameter 5cm is annealed to reach t_2=45°C with the help of another hollow brass cylinder that was connected to a water thermostat by rubber hoses. The water thermostat's accuracy was 0.1°C. This takes about 6 min. Then the 45°C cylinder is quickly removed, measured sample with diameter 5cm and thickness about 2mm is placed on the top of the CBC and on the top of measured sample another hollow brass cylinder connected to another water thermostat with temperature t_1=25°C is placed. On the top a 100g weight was placed. The heat is being transferred from the CBC though the sample to colder brass cylinder (25°C). The temperature of the CBC is decreasing rapidly. The data acquisition of the decreasing temperature of the CBC is being done with the help of a thermocouple (type copper-constantan) that was connected to a National Instruments data acquisition equipment (NI USB-9211A, Portable USB-Based DAQ (Data Acquisition) for Thermocouples) that was connected to a computer by USB. Software LabVIEW Signal Express 2.5 was used for temperature data acquisition. Sampling period was set to 5s. The measurement took about 25 min. The non-linear analysis (exponential decay) of the time-temperature curve was performed.

Mathematical Model for the Measurement

For the derivation of mathematical model describing dependence of the temperature of the CBC on time we start with following heat balance.

$$-K\frac{dt}{d\tau} = \frac{S\lambda(t - t_1)}{\delta} + B(t - t_1) \tag{3}$$

where,

$t(\tau=0) = t_2 = 45°C$

K is the heat capacity of the CBC, central brass cylinder ($J\ K^{-1}$)

S is the sample area (m^2)

λ is the thermal conductivity ($W.m^{-1}.K^{-1}$)

t is acquired temperature of the CBC (°C)

t_1 is the temperature of hollow brass cylinder 25 (°C)

t_2 is initial temperature of CBC (°C)

δ is the thickness of the sample (m)

B is the coefficient accounting for a heat loss ($J.s^{-1}.\ K^{-1}$)

τ is the time (s)

B can be calculated according to

$$B = \alpha\, S_z \tag{4}$$

where α is heat transfer coefficient ($W.m^{-2}.K^{-1}$) and S_z is the heat loss area (m^2).

Right side of Equation (3) represents heat flow through the mass of the measured sample. The heat loss caused by natural flow of the air around the measuring instrument is accounted for.

We start with energy balance. Left side of Eq. (3) corresponds to immediate heat output of the central brass cylinder from initial t_2=45°C to the equilibrium temperature t_1=25°C. Thermal energy that is leaving the CBC is realized by two ways. Larger part occurs by conduction heat transfer through the measured sample. Smaller part is heat loss to the surrounding environment that is caused by natural air flow and also by radiation. This part of the equation is determined by so called "blind experiment" when instead of measured sample we place material with very small thermal conductivity. We have used expanded polystyrene with λ=0.035 W/mK. The importantis a good contact of the measured sample with both brasscylinders. In case of hard samples like PP we have to use special the normally conductive paste (alluminum powder in siliconeoil). In our case of EOC/graphite compositeswedid not have to use this special conductive paste because the samples were soft and the contact was perfect.

By solvingEq. (3) weget

$$t = t_1 - (t_1 - t_2) * e^{[-(A_1+A_2)\tau]} \tag{5}$$

where for A_1 and A_2 constants are given by Eq. (6) and (7).

$$A_1 = \frac{S\lambda}{\delta K} \tag{6}$$

$$A_2 = \frac{B}{K} \tag{7}$$

Practical calculation goes as follows. Eq. (5) can be simplified for the non-linear regression (exponential decay):

$$y = y_0 + ae^{(-bx)} \tag{8}$$

From a non-linear regression we get coefficient b. For example for pure EOC we got b=0.002382 (from Figure 2).

The heat loss from the instrument obtained by blind experiment is A_2 = 0.000368 s^{-1}. Thermal capacity of the central brass cylinder was K_1 = 94.107 J K^{-1}. Area of measured cylinder was S = 1.9635.10^{-3} m^2.

Then the thermal conductivity can be calculated as shown by Eq. (9) and (10).

$$A_1 = b - A_2 = 0.002382 - 0.000368 = 0.002014 \tag{9}$$

$$\lambda = \frac{A_1 \delta K_1}{S} = \frac{0.002014 * 0.002305 * 94.107}{\frac{\pi\, 0.05^2}{4}} = 0.196\, Wm^{-1}K^{-1} \quad (10)$$

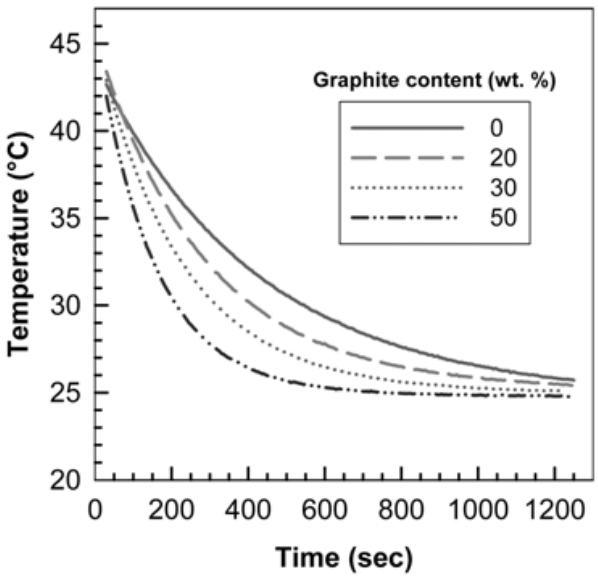

Figure 2. Thermal conductivity measurement: raw data. Temperature as a function of time for EOC/graphite composites with various graphite content. Initial temperature was 45°C and equilibrium temperature was 25°C. Sample had diameter 50 mm and thickness about 2 mm.

Flammability Test

Horizontal flammabilty test was carried out according to the UL-94 standard. Burner with yellow-tipped blue flame of 20 ± 1 mm height was used for the test. Samples were held horizontally at an angle of 45° and ignited using the flame for 30 ± 1 seconds. Samples had two marks; one at 25 mm and another at 100 mm. Test was conducted for three specimens in each category.

Shore-A hardness

Hardness of the EOC/expandable graphite composites has been measured using Bareiss Shore-A hardness tester (Model HHP-2001).

RESULTS AND DISCUSSION

Morphology of Composites

Flakes-like structure of the expandable graphite filler is clearly shown in Figure 3a. Morphology of the composites, displayed in Figure 3b, 3c and 3d, helps us to understand the

distribution of expandable graphite flakes in the polymer matrix. There are three micrographs of composites shown here: one below percolation threshold (3b), one around (3c) and the third one (3d) above the percolation threshold. One can observe increasing amount of graphite particles in the composite (3b→3d), with uniform dispersion of the particles which implies thorough mixing.

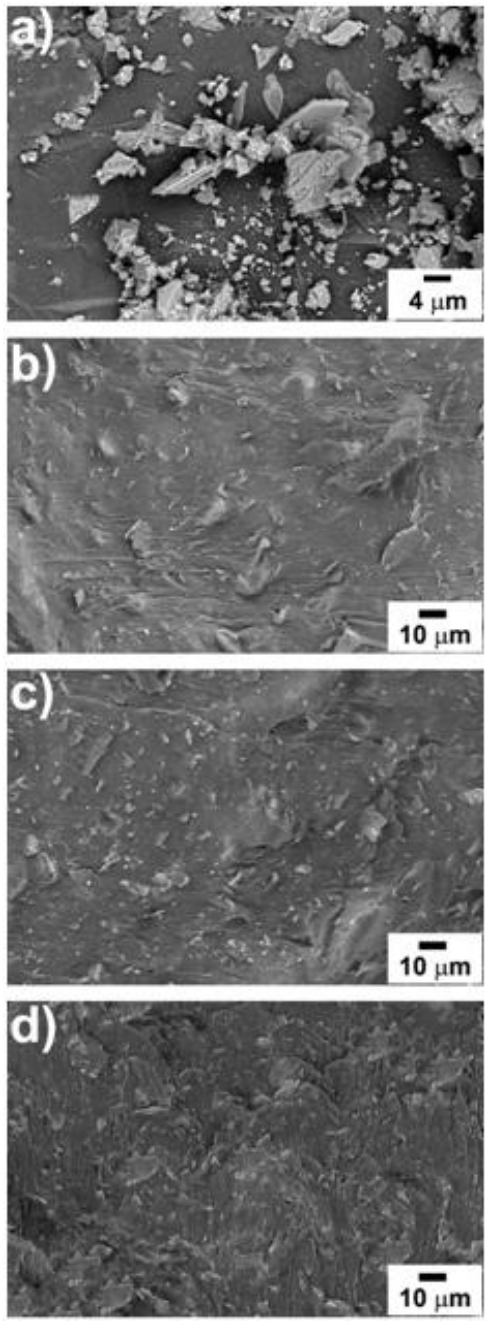

Figure 3. SEM micrographs of (a) Expandable graphite and EOC/expandable graphite composites with (b) 20, (c) 30 and (d) 40 wt. % of filler.

DC Conductivity (σ_{DC})

Conductivity of polymer composites with conducting fillers is greatly affected by filler loading level and distribution or filler alignment in the matrix. Figure 4 shows the dependence of DC conductivity on graphite level. It is very clearly visible from the plot that a sharp increase in the conductivity at particular filler level called percolation threshold. At and above this level, free movement of charge carriers makes the system more conductive or in other words, continuity between the conducting graphite flakes is created. Below percolation threshold, for example, at 5% graphite level, the conductivity is only 1.5 x 10^{-13} S cm^{-1}. Here, conductive paths were not developed and the conductivity may be due to that of ionic conductivity of the polymer composite. From the graph, one can estimate that the percolation threshold lies around 30 wt. % (or 16 vol. %) of graphite loading, where conductivity shows a sharp increase. For a mathematical model system of conducting spheres, randomly distributed in a non-conducting matrix, percolation at 16–17 vol. % was calculated [30]. And our value of percolation level is in good agreement with this model. Above percolation threshold, amount and distribution of filler increases and thus conductivity becomes easier. Small value of the deviations reveals good homogeneity of polymer composite systems, which is also supported by the SEM micrographs of the composites.

The relation of conductivity, σ with volume fraction of the filler can be explained by the power law model of conductivity [15] which is given as:

$$\sigma = \sigma_0 (\phi-\phi_c)^t \tag{11}$$

where, $\sigma_0$is the conductivity of the filler (1.33x10^4 Scm^{-1}, in the case of graphite flakes), ϕ is the volume fraction of the filler, ϕ_c is the critical volume fraction and t is the universal exponent determining the power of the electrical conductivity increase above ϕ_c.

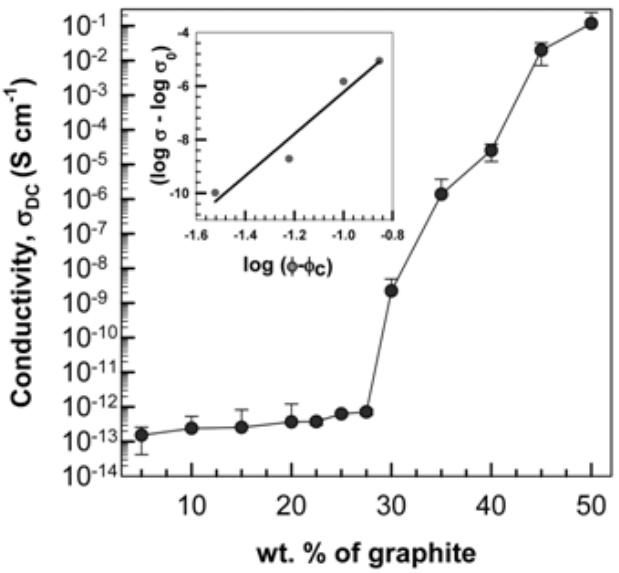

Figure 4. Dependence of DC conductivity on graphite content.

The plot of (log σ- log σ_0) versus log(ϕ-ϕ_c) is shown as an inset in the Figure 4. Slope of this curve gives the value of t. Calculated value of t from previous research was found to be in the range of 1.5 - 2.0 [31], in our case t=1.77, which is in good agreement with the literature.

AC Conductivity (σ_{AC})

Dielectric properties of EOC/graphite composites were measured in an alternating electric field. Dependence of AC conductivity on frequency is shown in Figure 5.

According to Eqn. (1), AC conductivity, σ_{AC}, is proportional to imaginary part of permittivity and frequency. As the frequency increases, AC conductivity also increases, according to Equation (2).

For lower concentrations (20, 25, 30 wt.%) the AC conductivity is increasing with frequency, therefore conductivity is provided by polarization current of fixed dipoles. AC conductivity in the low frequency region have some relations with DC conductivity. Above percolation level (35-40 wt.%), at low frequencies, the plateau relates to the values of DC conductivity, which is in good agreement with results determined by DC conductivity measurements. Similar observations were made by other researchers also [32].

AC conductivities of all compositions at four selected frequencies, 10^3, 10^6, 10^7 and 10^9Hz, are shown in Figure 6. As the frequency increases, percolation behaviour in the 30-35 wt. % graphite range is not so prominently seen like in the case of low frequencies and almost disappears at high frequencies. At high frequencies, rather than percolation, there is a gradual increase in AC conductivity with increasing graphite content. It shows the effect of frequency on the AC conductivity.

In the case of composites with 10 – 50 wt.% of graphite, at low frequency, conductivity increases from 10^{-11} to 10^{-2} Scm^{-1}; we can observe an increment of 9 orders. But at higher frequency, this rise ranges only from 10^{-3} to 1 Scm^{-1}, only of 3 orders.

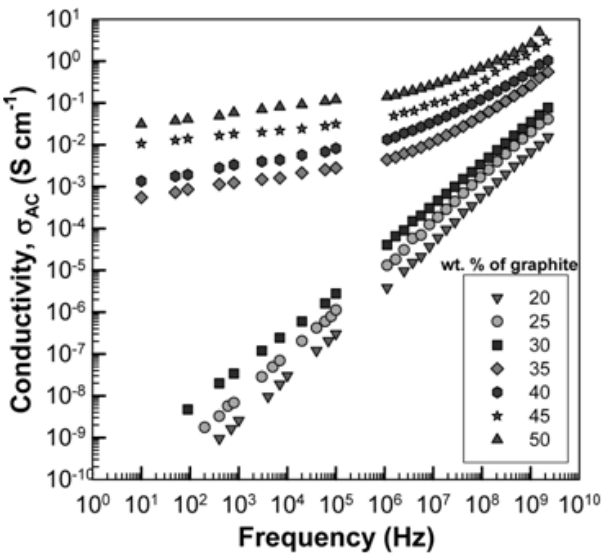

Figure 5. AC conductivity vs. frequency of EOC/graphite composites.

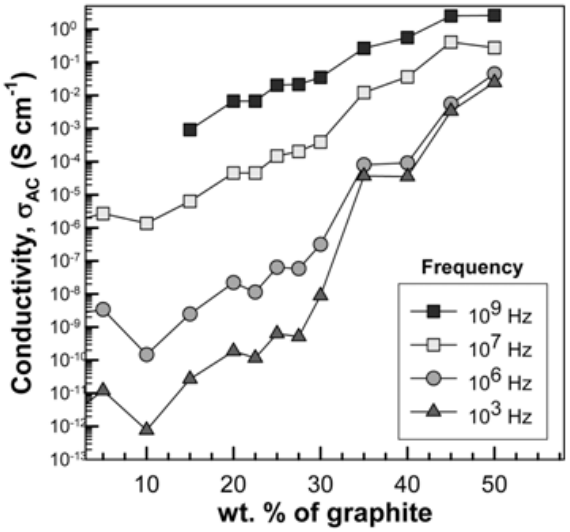

Figure 6. AC conductivity as a function of graphite content at different frequencies.

Dielectric Constant (ε′)

As shown in Figure 7, for filler content 0-30 wt. %, ε′ value is equal to around 10^1 and for filler content above 30 wt. %, ε′ value is around 10^7 at the frequency 10^1 Hz and it is illustrated that as the filler content increases, ε′ value also increases. As the frequency increases, permittivity decreases. This can be attributed to the interfacial polarization (IP) of the filler. At low frequencies, all types of polarization contribute to the resulting value of permittivity, in our case predominantly interfacial polarization, typical for systems containing phases of different specific conductivity.

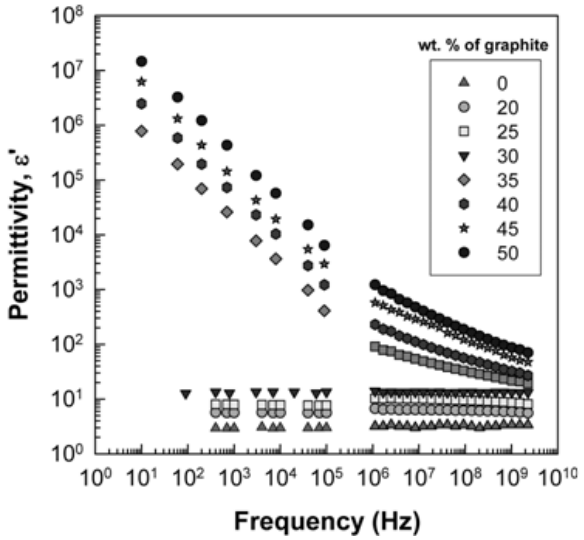

Figure 7. Real part of permittivity as a function of frequency.

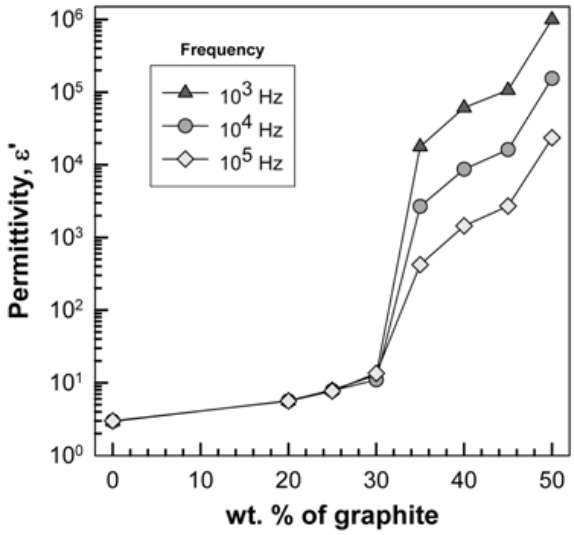

Figure 8. Permittivity as a function of graphite content at different frequencies.

IP arises in electrically heterogeneous materials such as composites and known as the Maxwell-Wagner-Sillars (MWS) effect [20]. The IP leads to an increase in ε' due to the motion of virtual charges, which get trapped at the interface of components of a multiphase material of different conductivity [33]. Similar observations have been made by Paul and Thomas [6]. Permittivity as a function of graphite content is shown in Figure 8. As in the case of conductivity, percolation behavior at low frequencies (10^3 Hz) is more prominent than at higher frequencies.

Thermal Conductivity (λ)

Thermal conductivity as a function of graphite content is given in Figure 9. As it can be seen from the figure, thermal conductivity increases as the filler content increases. Thermal conductivity of pure EOC matrix was found to be 0.196 W $m^{-1}K^{-1}$ while a 30 wt.% graphite loading increased the value almost 100% to 0.393 $Wm^{-1}K^{-1}$ and for 50 wt.%, the λ value was 0.676 W $m^{-1}K^{-1}$ i.e. about 245% increase.

Uniform dispersion of the filler has high influence on the increase in thermal conductivity as in the case of electrical conductivity. Since graphite is good conductor of heat and electricity, the increase in graphite level will result in an increase in electrical and thermal conductivities of the EOC/graphite composites.

Flammability Testing

Flammability test (Horizontal Burning - HB classification) was carried out according to the UL-94 standard. Composites with graphite loading less than 40 wt. % burnt all the way up to the holder. Only samples with filler loading 40, 45 and 50 wt. % did not burn to the holder, the flame self-extinguished.

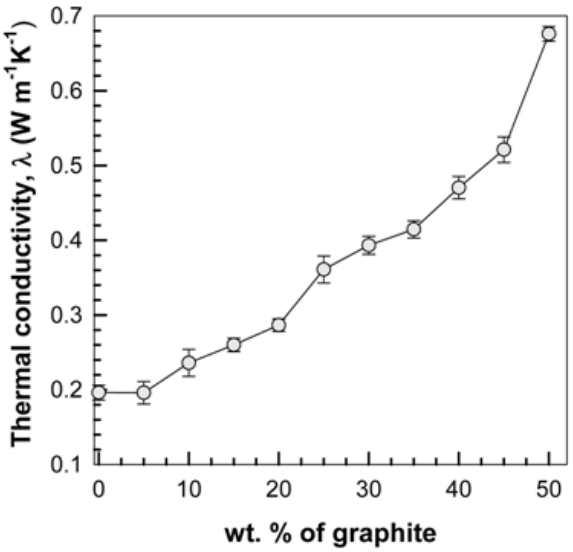

Figure 9. Thermal conductivity as a function of graphite content.

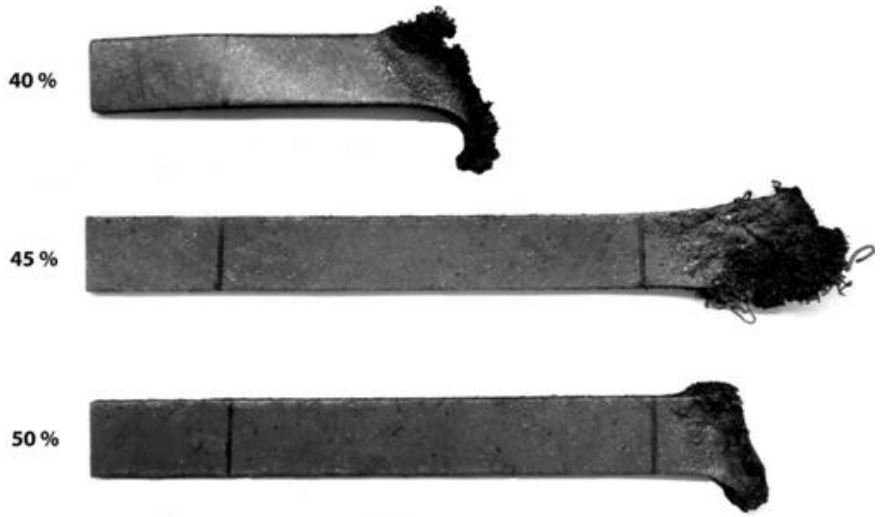

Figure 10. Samples with 40, 45 and 50 wt. % of graphite after horizontal flame testing.

Photograph of these three specimens is given in Figure 10. The EOC/graphite composites can be classified as HB according to the UL-94 standards since their burning rates did not exceed 75 mm min^{-1}, the maximum burning rate was found to be 47 mm min^{-1}.

Shore-A hardness

Composites of soft matrix polymers with conducting fillers are being used as strain or pressure sensors [34]. Thus hardness of these composites has practical importance. Shore-A hardness of the graphite/EOC composites has been measured and it was found to be increasing with increasing graphite content. See Figure 11.

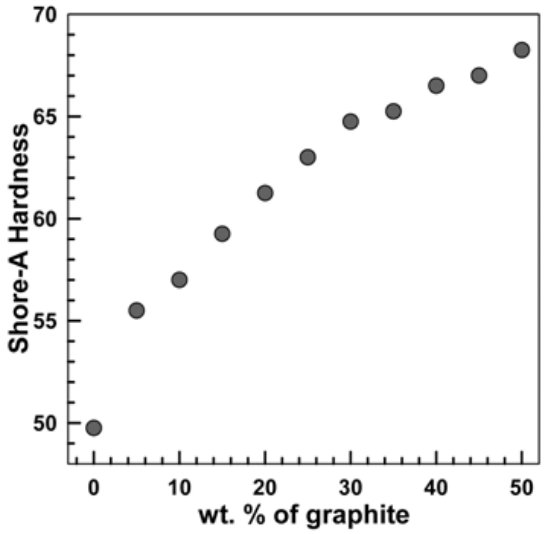

Figure 11. Shore-A hardness as a function of graphite content.

Shore-A hardness of pure EOC matrix was 50 while addition of 5% graphite increased the value to 55. Even the addition of 50 wt. % of graphite resulted in a hardness value of only 68. This shows that hardness of EOC/expandable graphite composites did not increase markedly with the addition of graphite filler, or in other words higher loadings of graphite did not hamper the rubbery nature of the EOC matrix. This is important in case of applications involving sensors when the electric conductivity is changing with pressure [34]. This will be the subject of our future study.

The softness of the composite was important also for the measurement of thermal conductivity. Very hard samples such as polypropylene (PP) might not have flat surface (especially after injection molding). Rough surface creates an air gap between the sample and the conducting metal. When the sample is soft, there is no such air gap, rendering perfect contact which assures proper thermal conductivity measurement.

CONCLUSION

Both AC and DC conductivities of EOC/graphite composites were found to be increasing with increase in graphite content. Percolation threshold has been observed at about 16 vol. % in both cases (DC and AC conductivities). Thermal conductivity of the composites showed a trend of increment with addition of graphite filler, but no percolation threshold was observed. Horizontal flame test according to the UL-94 standard proved the role of expandable graphite filler as an environmentally friendly halogen-free flame retardant. EOC composites with graphite content higher than 40 wt. % (or 22 vol. %) showed self-extinguishing behavior during horizontal flame test. Higher loadings of expandable graphite filler did not cause serious reduction in rubbery nature of the EOC/expandable graphite composites which could be potentially used in applications like pressure or temperature sensors. In summary these composites possess good electrical and thermal conductivities together with significant flame retardancy at higher loadings without extreme increase in hardness values.

APPENDIX

Since there is a possibility to use these composites in automotive industry and in electronics because of acceptable flame resistance the burn rate was examined in detail. Figures 12-15 show the horizontal burn tests with the evaluation of burn rate. When we compare Figures 12 and 13 it is clear that it takes longer to burn the sample with 30 wt.% of graphite.

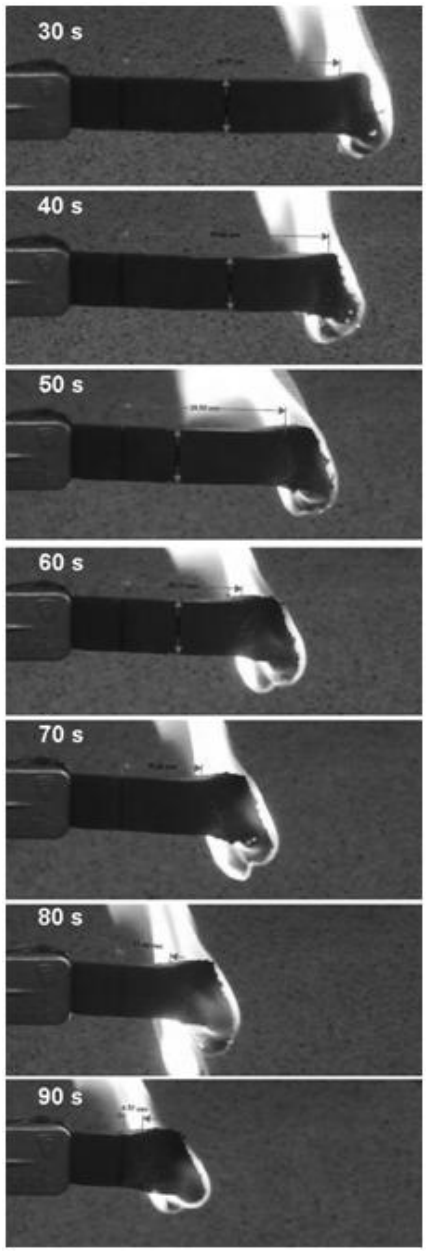

Figure 12. Horizontal burn test of EOC with 20 wt.% of graphite.

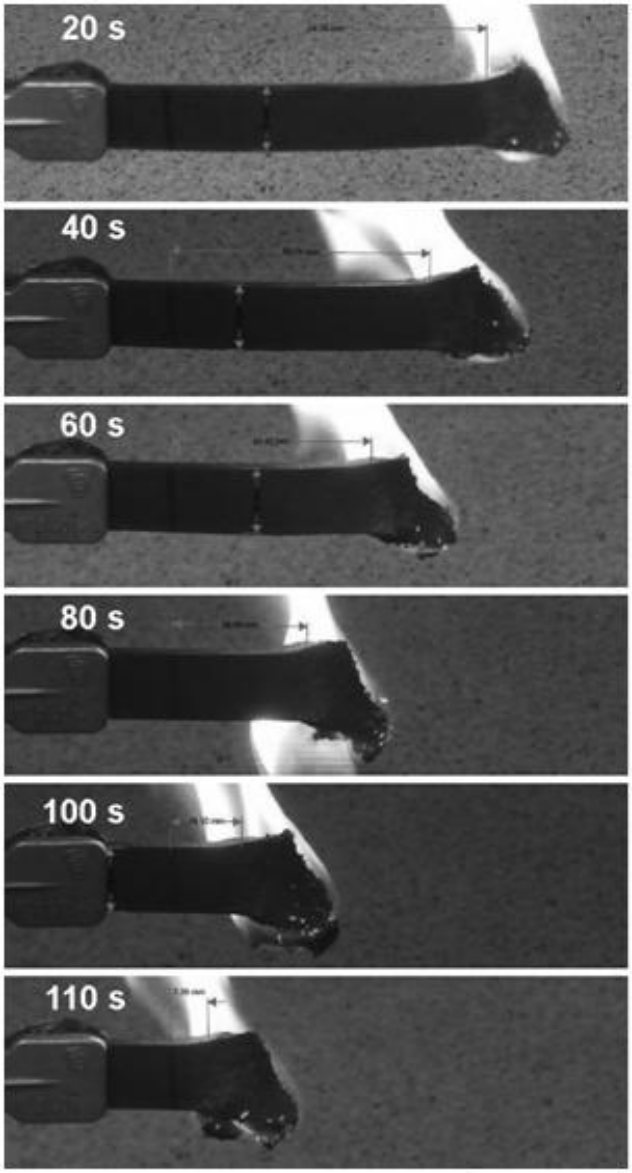

Figure 13. Horizontal burn test of EOC with 30 wt.% of graphite.

When we plot the distance that the flame travels as a function of time we can get a plot that is illustrated on Figure 14. When one evaluates the slope of the line it is possible to get a burn rate. This burn rate was plotted as a function of graphite content on Figure 15. Very interestingly initially the rate increases with increasing graphite content (up to 30 wt. % of graphite).

It is possible to explain this phenomenon by increasing thermal conductivity (shown on Figure 9). The heat travels faster when there is more graphite present. However at concentrations higher than 20 wt.% the influence of graphite as flame retardant prevails over the increased thermal conductivity effect. There is a visible decrease in burning kinetics when the concentration is increased from 20 to 30 wt.% of graphite.

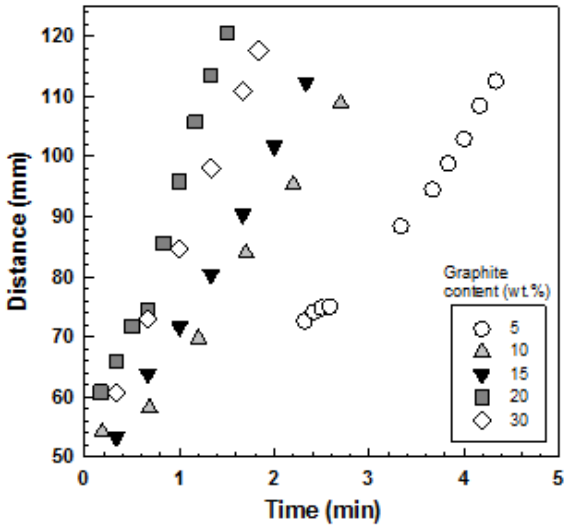

Figure 14. Evaluation of the burn rate during the horizontal burn test.

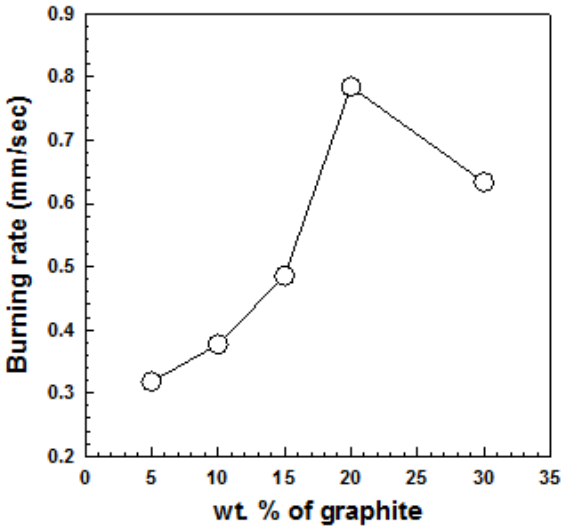

Figure 15. Burning rate as a function of graphite content.

The decrease in burn rate continues even more at concetntrations 40-50 wt.% as was shown on Figure 10 when the samples actually self-extinguished during the tests (therefore we could not evaluate the burn rate).

ACKNOWLEDGMENTS

This work has been supported by Operational Programme Research and Development for Innovations co-funded by the European Regional Development Fund (ERDF) and national budget of Czech Republic within the framework of the Centre of Polymer Systems project (reg.number:CZ.1.05/2.1.00/03.0111).

REFERENCES

[1] V.S. Mironov, J.K. Kim, M. Park, S. Lim, W.K. Cho, *Polym.Test*., 26, 547–555 (2007).
[2] Q. Zhang, H. Xiong, W. Yan, D. Chen, M. Zhu, *Polym. Eng. Sci.*, 48, 2090 - 2097 (2008).
[3] Q. Chen, Y. Xi, Y. Bin, M. Matsuo, *J. Polym. Sci. Pol. Phys.*, 46, 359-369 (2008).
[4] J. Vilcakova, P. Saha, O. Quadrat, *Eur. Polym. J.*, 38, 2343-2347 (2002).
[5] W.-y. Wang, G.-h.Luo, F. Wei, J. Luo, *Polym. Eng. Sci.*, 49, 2144-2149 (2009).
[6] A. Paul, S. Thomas, *J. Appl. Polym. Sci.*, 63, 247-266 (1997).
[7] R.K. Goyal, S.D. Samant, A.K. Thakar, A. Kadam, *J. Phys. D. Appl.Phys.*, 43, 1-7 (2010).
[8] N.M. Renukappa, Siddaramaiah, R.D.S. Samuel, J.S. Rajan, J.H. Lee, *J. Mater. Sci.-Mater. El.*, 20, 648-656 (2009).
[9] H. Kim, A.A. Abdala, C.W. Macosko, *Macromolecules*, 43, 6515–6530 (2010).
[10] S. Bhadra, N.K. Singha, D. Khastgir, *Polym. Eng. Sci.*, 48, 995-1006 (2008).
[11] S. Hom, A.R. Bhattacharyya, R.A. Khare, A.R. Kulkarni, M. Saroop, A. Biswas, *Polym. Eng. Sci.*, 49, 1502-1510 (2009).
[12] J.-C. Huang, H.-L. Huang, *J. Polym. Eng.*, 17, 213-229 (1997).
[13] W.-P. Shih, L.-C.Tsao, C.-W.Lee, M.-Y.Cheng, C. Chang, Y.-J.Yang, K.-C. Fan, *Sensors*, 10, 3597-3610 (2010).
[14] S.A. Mansour, *eXPRESSPolym. Lett.*, 2, 836-845 (2008).
[15] S. Kirkpatrik, *Rev. Mod. Phys.*, 45, 574-588 (1973).
[16] Y.R. Hernandez, A. Gryson, F.M. Blighe, M. Cadek, V. Nicolosi, W.J. Blau, Y.K. Gun'ko, J.N. Coleman, *Scripta Mater.*, 58, 69-72 (2008).
[17] M.H. Al-Saleha, U. Sundararaj, *Carbon*, 47, 2-22 (2009).
[18] W. Zhang, A.A. Dehghani-Sanij, R.S. Blackburn, *J. Mater. Sci.*, 42, 3408-3418 (2007).
[19] R. Strumpler, J. Glatz-Reichenbach, *J. Electroceram*., 3, 329-346 (1999).
[20] H. Hammami, M. Arous, M. Lagache, A. Kallel, *J. Alloy. Compd.*, 430, 1-8 (2007).
[21] X.Y. Meng, L. Ye, X.G. Zhang, P.M. Tang, J.H. Tang, X. Ji, Z.M. Li, *J.Appl. Polym. Sci.*, 114, 853-863 (2009).
[22] X.L. Chen, J. Yu, S.J. Lu, H. Wu, S.Y. Guo, Z. Luo, *J. Macromol. Sci. Part B-Phys.*, 48, 1081-1092 (2009).
[23] C.-H. Chen, W.-H.Yen, H.-C.Kuan, C.-F.Kuan, *Polym. Composite*., 31, 18-24 (2010).
[24] C.-L. Chiang, S.-W. Hsu, *J. Polym. Res.*, 17, 315-323 (2010).
[25] B.J. Qu, R.C. Xie, *Polym. Int.*, 52, 1415-1422 (2003).
[26] H. Fukushima, L.T. Drzal, B.P. Rook, M.J. Rich, *J. Therm. Anal. Calorim.*,85, 235-238 (2006).
[27] L.J. Van der Pauw, *Philips Res. Rep.*, 13, 1-9 (1958).
[28] F.G.d.S. Jr., B.G. Soares, J.C. Pinto, *Eur. Polym. J.*, 44, 3908-3914 (2008).
[29] J.E. Lozano, *Fruit Manufacturing: Scientific Basis, Engineering Properties and Deteriorative Reactions of Technological Importance*, Springer Science Business Media LLC., New York, (2006).
[30] H. Scher, R. Zallen, *J. Chem. Phys.*, 53, 3759-3761 (1970).
[31] N.K. Srivastava, V.K. Sachdev, R.M. Mehra, *J. Appl. Polym. Sci.*, 104, 2027-2033 (2007).

[32] M. Pelíšková, J. Vilčáková, R. Moučka, P. Sáha, J. Stejskal, O. Quadrat, *J. Mater. Sci.*, 42, 4942-4946 (2007).
[33] F. Kremer, A. Schonhals, *Broadband Dielectric Spectroscopy*, Springer-Verlag, Berlin Heidelberg, (2003).
[34] S. Bhadra, N.K. Singha, D. Khastgir, *Curr. Appl. Phys.*, 9, 396–403 (2009).